DANMARKS OG GRØNLANDS GEOLOGISKE UNDERSØGELSE RAPPORT 2001/125

Geodynamic and petrophysical modelling in the Kraka area

Peter Frykman

GEOLOGICAL SURVEY OF DENMARK AND GREENLAND
MINISTRY OF ENVIRONMENT AND ENERGY

G E U S

DANMARKS OG GRØNLANDS GEOLOGISKE UNDERSØGELSE RAPPORT 2001/125

Geodynamic and petrophysical modelling in the Kraka area

Report for EFP-2001 project "Modelling of dynamic fluid contacts in chalk reservoirs" ENS J.nr. 1313/01-0004

Peter Frykman

GEOLOGICAL SURVEY OF DENMARK AND GREENLAND
MINISTRY OF ENVIRONMENT

G E U S

Geodynamic and petrophysical modelling in the Kraka area

Introduction

The present report has been prepared with the aim of presenting a model for the burial history of the chalk section in the Kraka field based on seismic mapping, data from wells, backstripping and decompaction. The model records the burial history of the chalk section in an area around the Kraka field. The parameters and models for the petrophysical properties are also presented in the perspective of being usable in the dynamic modelling.
The present geological model is based on data originating from an existing study (Salinas *et al.* 1994), and does therefore not include more recent well data or additional seismic data. The present model is intended to be used for initialising the development of geodynamic flow modelling, and the model will therefore be updated and refined as the project progresses.
The Kraka field was discovered in 1966 (A-1X well) and was declared commercial in 1985. Development commenced in 1991.
Kraka was in 1993 estimated to contain 31.7 mio.m^3 (st) (200 MMstb) of 31.5 API oil initially (Thomasen & Jacobsen 1994), but this value is uncertain due to uncertainty in the interpretation of the top structure map and in the complex geometry of the fluid contacts. The initial pressure at the gas-oil contact GOC was 3640 psia (5852 feet ss (TVD m.s.l.) (Thomasen & Jacobsen 1994).
The Kraka field is situated in the southern part of the Central Graben in the Danish sector of the North Sea. It is a large, elongate dome at Top Chalk level.

Structural setting

The Kraka field is located in the southern part of Central Graben in the Danish North Sea sector, just south of the Dan field (Fig. 1). The Kraka field is a relatively simple structural dome (Fig. 2) situated in the Southern Salt Dome Province, above a Zechstein evaporitic accumulation, which started halokinesis in the Triassic and was remobilized during the late Kimmerian tectonic pulse (Jørgensen 1993).

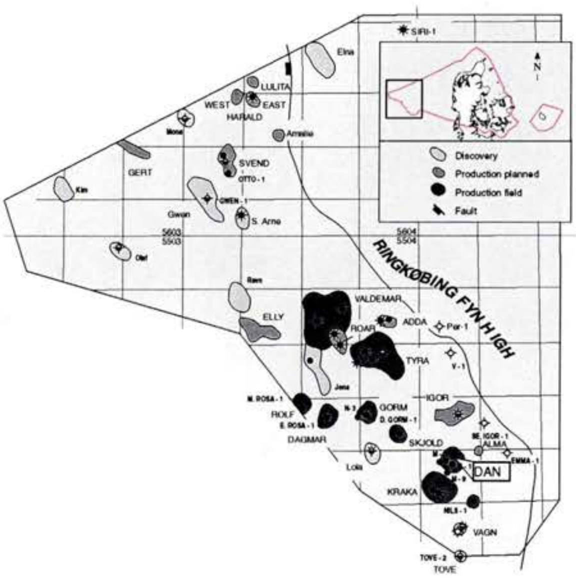

Fig. 1 – Map of the Danish North Sea showing the fields in production.

The long axis of the domal structure is 8 km, and the short axis is 5 km. Vertically the relief is 500 ft (150 m) from the lowest closing contour of the Dan field to the top of the structure. The flanks dip less than 5 degrees.

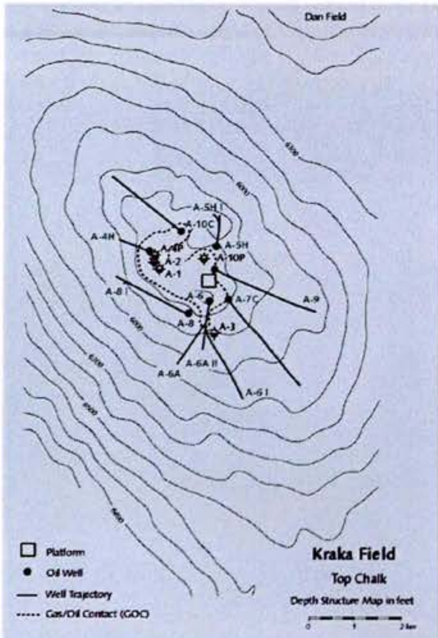

Fig. 2 - The Kraka field with well positions (Danish Energy Agency 2001).

Wells in the Kraka field

The following wells are presently drilled in the Kraka structure: A-1X, A-2X, A-4P and A-4H in the north western part of the structure; A-5P and A-5H in the northern part; Anne-3 A-6, A-6I and A-6II in the southern part and the A-7C well in the south eastern flank. Three additional wells A-8, A-9 and A-10 have been drilled during 1994 and 1997.

The wells in the Kraka field have over time been known by different names which has caused confusion as to whether the abbreviation is referring to a side-track, pilot-hole or horizontal part. A table listing the well names and other attributes is given in appendix.
The first well in the Kraka field (A-1X) was drilled in 1966 slightly north west of the top of the structure. After penetrating 80 ft below the Top Chalk surface, the well was suspended due to technical problems (Jørgensen & Andersen 1991). However, the well did reveal the first oil and gas discovery in the North Sea chalk area during 1966.

Fluid contacts

Dipping fluid contacts have been recognised early as being a result of the hydrodynamic gradient (Jørgensen & Andersen 1991; Megson 1992; Thomasen & Larsen 1994). Using RFT pressures from three Kraka wells, the FWL was mapped and shown to dip 0.63 degrees at a southeasterly azimuth, corresponding to a change in FWL level of 300 feet across the accumulation. The water pressure gradient across the Kraka structure is 10 psi/km corresponding to an average water velocity of 4 mm/year (Thomasen & Jacobsen 1994).

Geophysics

Introduction

The Kraka 3D seismic survey was acquired as part of Phase 1 of the 1988 Kraka Field Development Plan. The interpretation of the 3D seismic survey provided input to the structural mapping and the modelling of the burial history and backstripping of the Kraka field.

Seismic Data

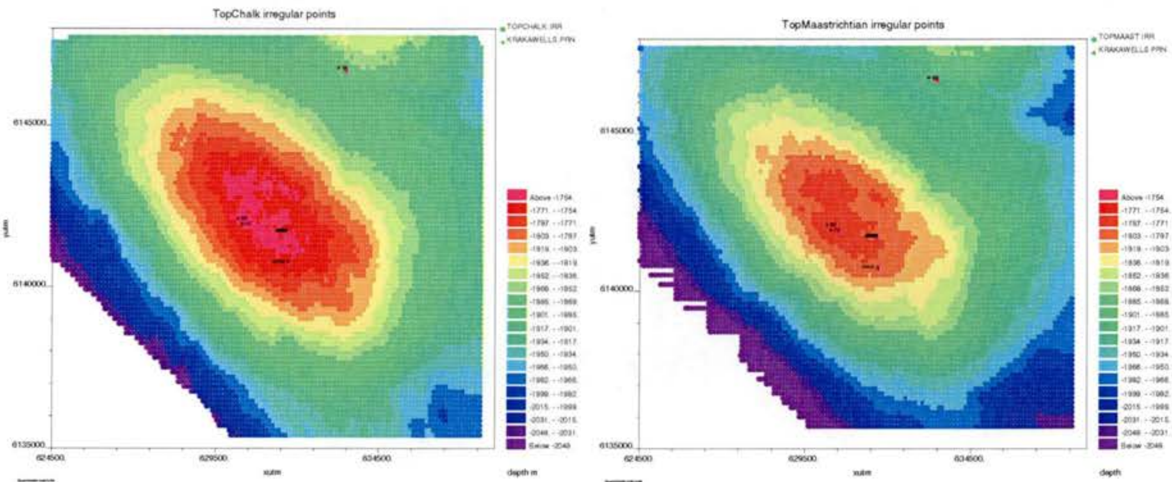

Fig. 3, 4 – The data available for the mapping of top Chalk and top Maastrichtian. Wells are shown with their well-head UTM coordinates. The 3D survey covers an area of approximately 13x13 km. The uncertainty in the SW area is due to lack of seismic coverage, and is therefore extrapolated in the mapping of the structural maps.

Well Data

Data from 8 wells and their side-tracks were used during the interpretation of the Kraka 3D seismic survey and the structural mapping in the area.
The well data base consists of the following wells:

1. A-1X
2. A-2X
3. Anne-3
4. A-4P, A-4H
5. A-5P, A-5H
6. A-6P, A-6A, A-6I, A-6II
7. A-7, A-7A, A-7B, A-7C
8. M-8X, M-9X (Dan Field)

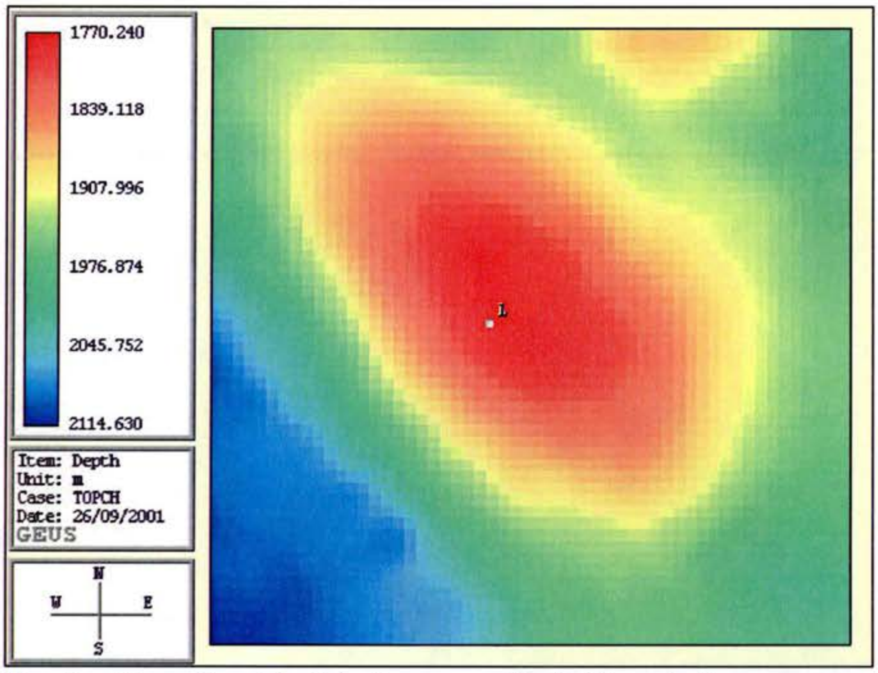

Fig. 3 – Map of top Chalk in the area with A-1X posted.

Only two of these wells (A-2X and Anne-3) penetrate the entire chalk sequence. In the A-2X there is only log data from the upper part of the Chalk Group. Calibrated sonic log data is limited in the area since most of the logs cover only parts of the hole from surface down to the Maastrichtian chalk.

M-9X (Fig. 4) was the key well for the stratigraphic identification of the seismic events and provided a good tie to the seismic data. However, formation tops and log data from the other wells were used during the correlation between seismic and well data.

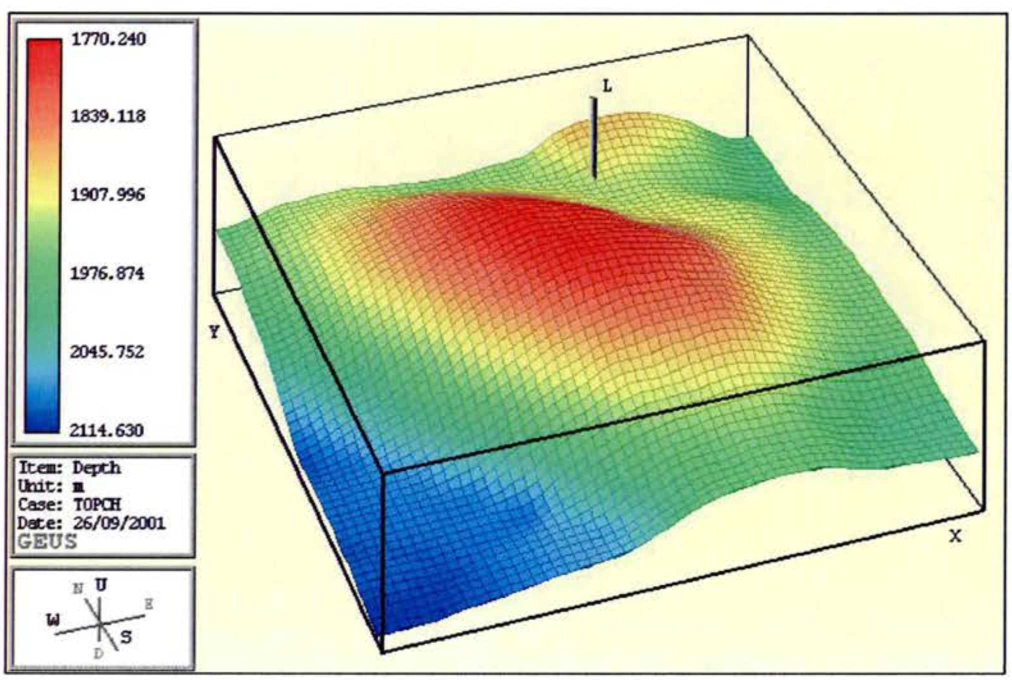

Fig. 4 – Map with depth to top chalk and the well M-9x on the southern flank of the Dan field posted.

A large number of arbitrary well-tie lines were constructed through the seismic data cube to help identify the horizons away from the well locations. The reflector strength and continuity of the Quaternary and Tertiary horizons are generally high.
The Top Chalk Group reflector shows a phase reversal over the gas saturated area. Phase and amplitude distortion on the seismic data is also observed beneath the gas cap where the seismic response of hydrocarbon contact masks and /or interferes underlying reflectors.

Structural Mapping

Twelve horizons have been interpreted within the 3D data cube and have been tied to the wells A-2X and M-9X. Data for TWT are listed in the appendix.

The maps exhibit low structural complexity in the area, especially at post-chalk levels. A low relief structure is mapped at chalk level. A number of isotime maps were constructed, and indicates that the Danian Chalk isotime is thickening towards south-south east.
All the above mentioned information was provided as input to the reconstruction of the structural growth history of the Kraka field in an attempt to build a tectonic and stratigraphic model of the reservoir.

Structural Growth History

Introduction

A study of the growth history for the Kraka Field has been performed. The purpose is to construct a geodynamic reservoir model of the field, and use this to investigate the movement and distribution of fluids at different stages.
The methods, which are used are described in details in a previous report (Olsen 1993). Reference is made to that report for a description of the methods and the principles. Briefly, the method combines backstripping with forward modelling. This procedure as the first step determines the structural development during time from backstripping of the sequence. Then the forward modelling is used assuming a set of decompaction factors, until a match is obtained to the present day layer thickness and pressure distribution. The resulting set of decompaction factors describe the compaction of the layers after deposition in the forward modelling sequence.
The modelling has resulted in a burial history, including the development of the effective stress (Krogsbøll *et al.* 1995). This is shown for a well on the Dan Field in Fig. 5 as a comparison between the actual burial depth and the effective burial depth .

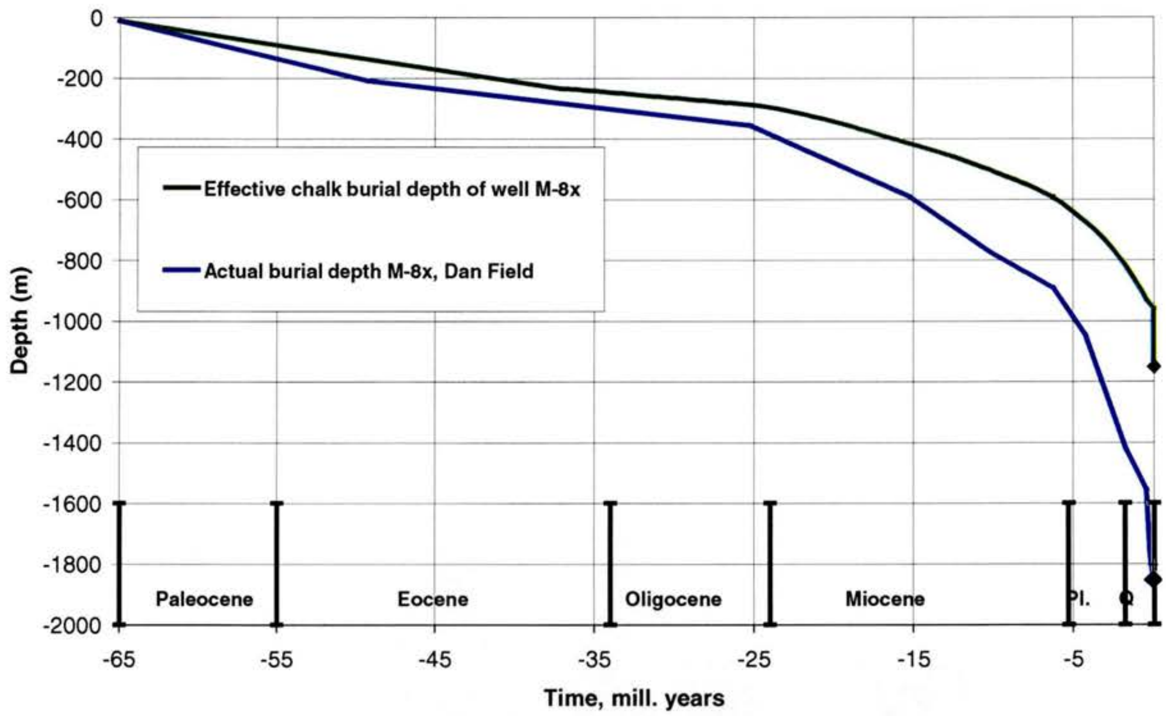

Fig. 5 – Comparison of the modelled actual burial and the effective burial depth when compensated for overpressure development. The separation between the two curves at an early stage before the major overpressure development is probably caused by uncertainty in the pressure modelling behind the effective stress calculations. The pressure modelling is very sensitive to the permeability model assumed for all the layers in the model. Data for stress and burial from existing study (Krogsbøll *et al.* 1995).

Forward Modelling of the Depositional History from previous work

For establishing a stratigraphy, seismic reflectors have been mapped, tied to the well data and dated. The post-chalk section has been divided into 14 layers. The appendix Table 3 lists the horizons, the layers and the dating of the horizons. The depths to the horizons in the A-2X well are listed also.

Following the backstripping and decompaction, different parameters have been simulated in four wells: M-9X, A-2X, ANNE-3 and A-5P.

Figure 6 shows the effective stress with time as simulated at the A-2X well location in a layer immediately above the Top Chalk level (Salinas *et al.* 1994). The effective stress is the difference between the total stress and the pore pressure. Figure 7 shows the excess pore pressure at the same level, also in A-2X. The excess pore pressure is the difference between the actual pore pressure and the hydrostatic pressure. It may be seen that both the effective stress and the excess pore pressure increase non-linearly with time. Because of this non-linearity the forward modelling method must be used to determine the compactional component of the deformations (Olsen 1993). Pressure data for different reservoirs are given in the Appendix.

A regional flow gradient has been taken into account in the modelling, having the same direction as in the Dan field; giving an OWC tilted at 155 degrees azimuth with an inclination of 14 m/km.

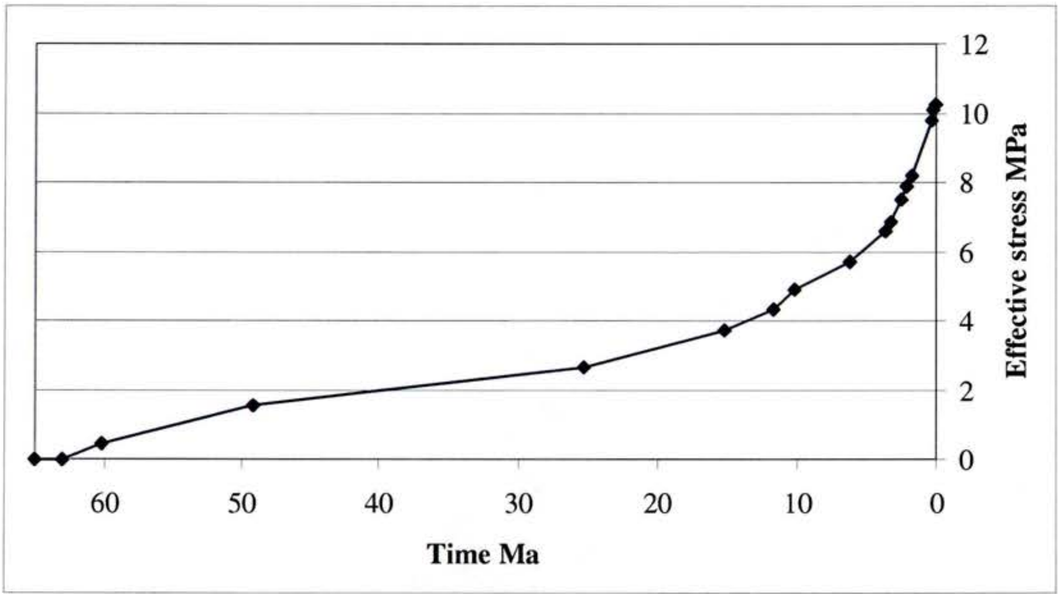

Fig. 6 – Effective stress through time at the A-2X well location in the layer immediately above the top chalk level. Data obtained and extended from existing Fig.93 in (Salinas et al. 1994).

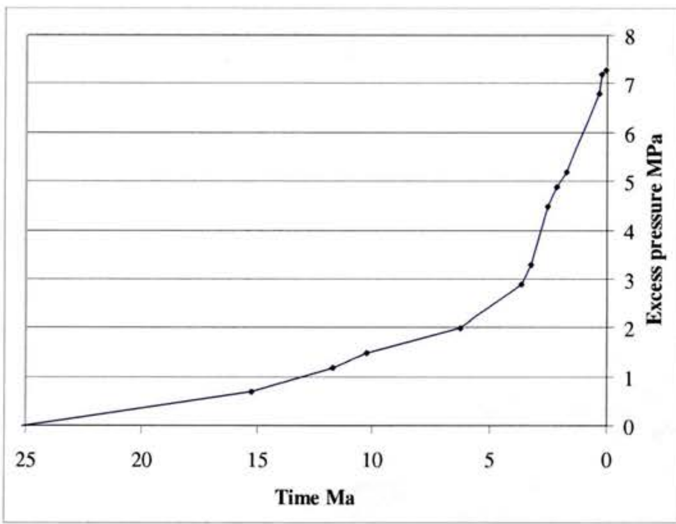

Fig. 7 – Excess pressure through time at the A-2X well location in the layer immediately above the top chalk level. Data obtained from existing Fig.94 in (Salinas et al. 1994).

The excess pressure is to be seen in connection with the hydrostatic and lithostatic gradient for the designated area. Gradient values are reported from the UK North Sea to be 10.0 KPa/m (Hy) and 23.0 KPa/m (Li) (Daniel 2001). For the Danish-Norwegian chalk province, the overburden material is less dense, and the overburden gradient is about 20.6 kPa/m (0.91 psi/ft) (Andersen 1995). The reservoir pressure is shown related to these two gradients (Fig. 8).

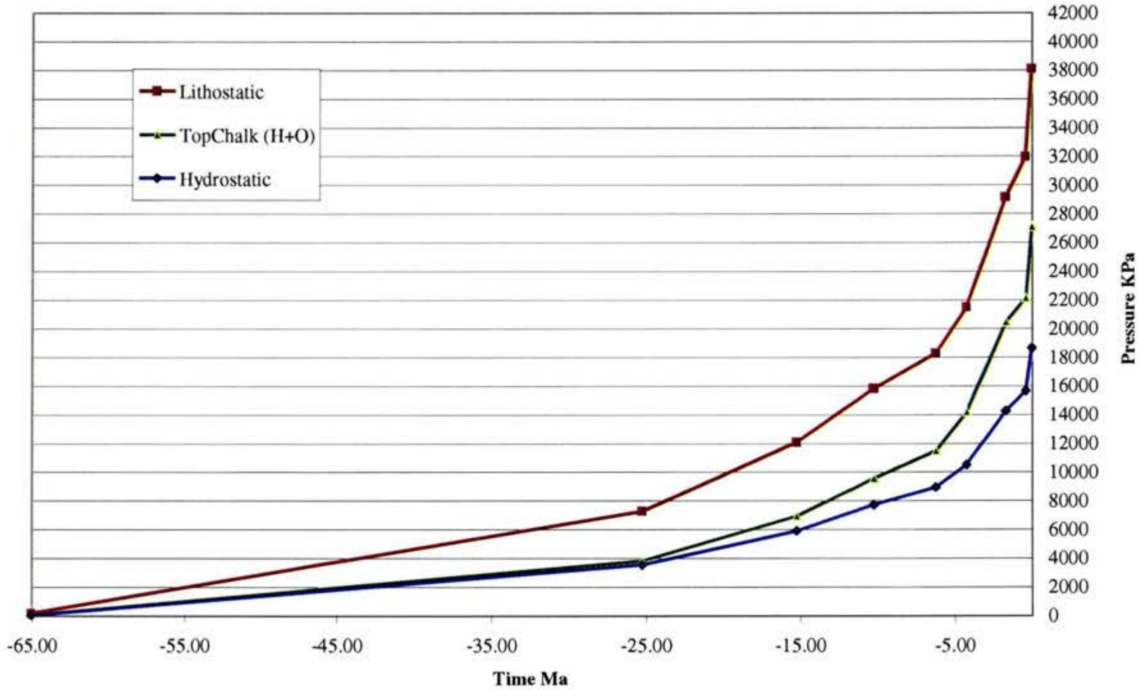

Fig. 8 – The simulated pressure development (Krogsbøll et al. 1995) compared to that of the hydrostatic and lithostatic gradients during time for the top chalk level in the M-8x well in the Dan field southern flank area. The overpressure is the difference between the Hydrostatic and the formation pressure. The modelled present overpressure is approx. 8.45 Mpa at top chalk level on the Dan field according to the modelling study, which is not matching the actual value of 6.4 Mpa given in Table 4 . The mismatch is due to uncertainty in the permeability modelling of the layers and the sensitivity of pressure to that permeability model.

The results from the depositional history modelling are decompaction factors, which describe the amount of compaction the layers have experienced during each depositional period.

Backstripping

The seismic reflectors (TWT) are transformed to depths (ft TVD) using the interval velocities from the M-9X well. These velocities are in accordance with the data from the A-2X well. The velocities are listed in table 4.

A single step in the backstripping procedure is carried out by removing the top layer followed by a decompaction of the remaining layers using the decompaction factors. The result is a geometrical model of the area at an earlier geological time. If the top chalk geometries corresponding to two different times are compared, a deformation field referring to that period is obtained. The deformation field describes the deformations caused by structural movements (Olsen 1993). The decompaction factors, initially determined at well locations (wells and pseudo wells) have been extrapolated to cover the model area. A general trend is that the decompaction factor is between 1.06 and 1.12 for the uppermost layer in each decompaction step, and between 1.02 and 1.05 for the rest of the layers in the sequence that is decompacted.

In the present study backstripping and decompaction has been carried out for 8 layers representing the last 11.7 mill. years. The results are 9 geometrical models of the area and 8 corresponding deformation fields. In addition two horizons for the TopLowerCen4 and

TopCen3 have been constructed by subtracting isopach maps for the layers UpperCen4 and LowerCen4, but excluding the step of decompaction. The Lower Cen4 isopach is purely artificial and does not match the horizon level in the well data. The results are evaluated and discussed in the following section.

Deformation history of the Kraka Structure

The deformation history of the Kraka Structure from Top Cen3 (25.2 mio years) to the present day situation is illustrated in Figs. 9 to 11. The figures show the structural position of the Top Chalk level at 10 time steps from 25.2 to 0.0 MA BP. The relative deformation of the Top Chalk surface for each of the 9 time intervals is shown in Fig.11. A geological evaluation of the 10 deformation fields is given below.

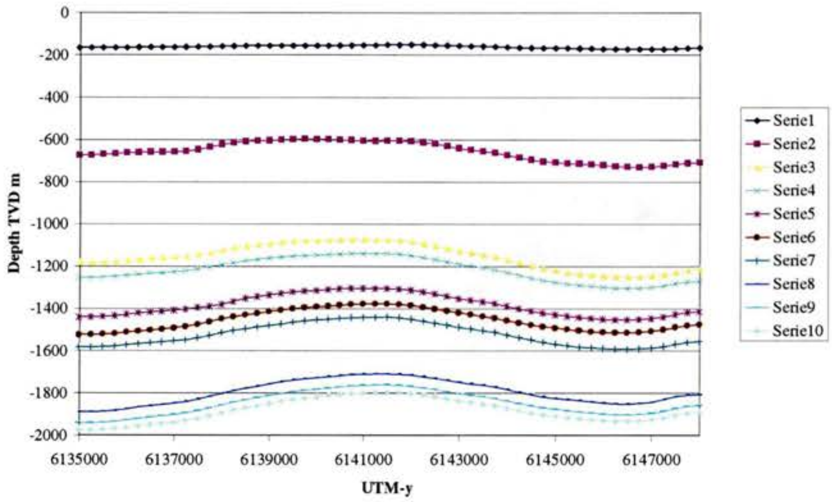

Fig. 9 – The top chalk surface during successive burial as seen in a N-S section in the middle of the mapped area. Topmost (serie1) is the top-chalk surface at 25.2 MA, then at 15.2, 3.6, 3.2, 2.5, 2.1, 1.7, 0.3, 0.17 and present depth.

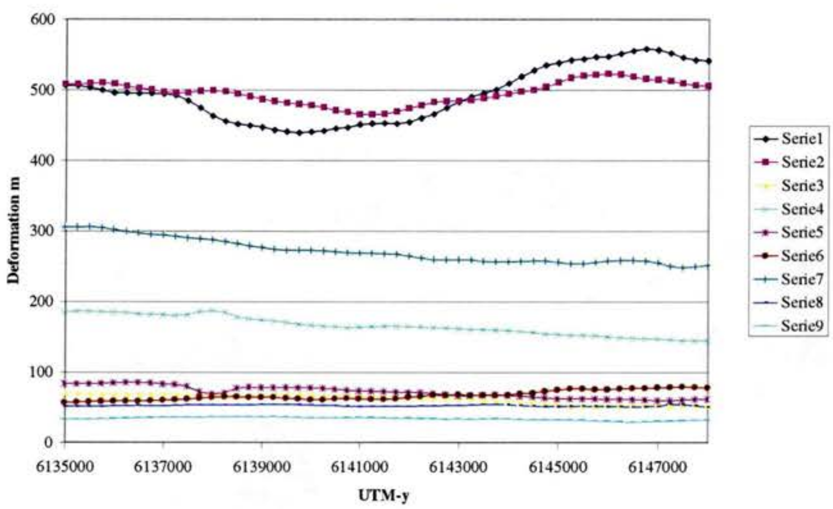

Fig. 10 – The amount of deformation during burial of the top chalk surface. Same section as in Fig. 9.

Possible errors /uncertainties concerning the deformation fields:

i) The available Kraka 3D seismic survey does not cover the southwesterly corner of the investigated area and horizons in this corner have therefore been extrapolated from the seismic interpreted of the covered area. The calculated deformation fields from this marginal area should therefore be viewed with some caution.

ii) the somewhat irregular curve pattern of the deformation fields is due to the fact that the seismic horizon interpretation has not been smoothed prior to the calculations.

iii) The presence of elongated local anomalies on several of the deformation fields does not reflect abnormal structural growth in these places, but are rather caused by seismic "push downs" and "pull ups" reflecting locally varying seismic velocities in Quaternary channel deposits. (Salinas *et al.* 1994).

iv) The earliest burial phase is modelled by a layer thickness that is not in accordance with some of the well data. However, this has very little influence on the important processes of porosity modifications during fluid movements which are starting at a later stage.

v) The seismic mapping and the dating of the horizons Cenozoic sequence is undergoing revision, and is also influenced by the non-layer-cake geometry in some of the layers where prograding sequences must be interpreted in more detail to assess the burial effects in time.

Evaluation of deformation fields

1st time interval, 60.2-25.2 MA BP (Fig. 11A - t12)
The deformation rate is small and fairly uniform.

2nd time interval, 25.2-15.2 MA BP (Fig. 11B)
The deformation is dominated by burial and some growth of the salt structure.

3rd time interval, 15.2-11.7 MA BP (Fig. 11C – t10)
Only slight deformation.

4th time interval, 11.7-3.6 MA BP (Fig. 11D – t01)
The deformation field is dominated by growth of the Kraka Structure and subsidence of the area ENE of the structure (alternatively tectonic tilt towards ENE). It is also seen that there is no relative growth of the Dan Structure in this period. These observations are in agreement with Dan Field results from an EFP-93 project (Krogsbøll *et al.* 1995).

5th time interval, 3.6-3.2 MA BP (Fig. 11 E – t02)
The subsidence of the easterly area continues, now in an ESE'erly direction. The growth of the Kraka and Dan salt domes has commenced. In fact, there appears to be a minor relative subsidence in the central part of the Kraka Structure.

6th time interval, 3.2-2.5 MA BP (Fig. 11 F – t03)
The deformation field has changed significantly, so that the relative subsidence (or tectonic tilt) is now towards SW. No relative structural growth of the salt domes is seen.

7th time interval, 2.5-2.1 MA BP (Fig. 11G – t04)
The overall picture of the deformation field is the same as above; subsidence towards WSW although at the same time there appears to be a reactivation of the growth of the Dan Structure.

8th time interval, 2.1-1.7 MA BP (=Top Tertiary)(Fig. 11H – t05)
The orientation of the relative subsidence has shifted slightly to a NWerly direction. No structural growth of the salt domes is seen.

9th time interval, 1.7-0.3 MA BP (Fig. 11I – t06)
The deformation field is now dominated by a reactivated structural growth of the Kraka and Dan structures. The subsidence of the westerly area is still seen.

10th & 11th time interval, 03-0.17 & 0.17-0.0 MA BP (Figs. 11J & K – t07 & t08)
Increased relative deformation rates of the chalk is seen in the SW area during the two youngest time intervals (late Quaternary).

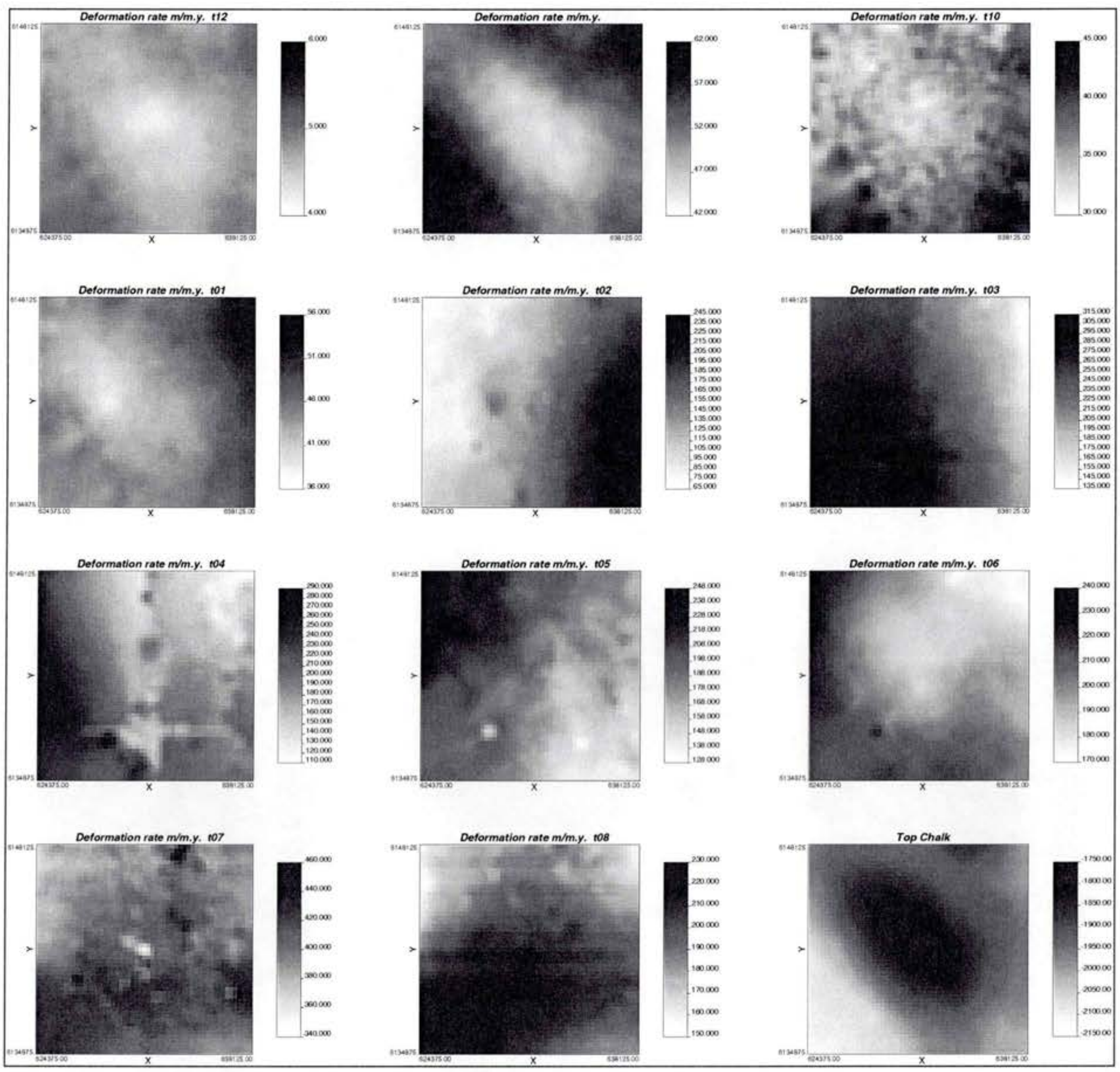

Fig. 11 – Maps of the deformation rate in each time interval for the successive mapped horizons, and a depth to top chalk map.

The development of the deformation rate is shown in Fig. 12.

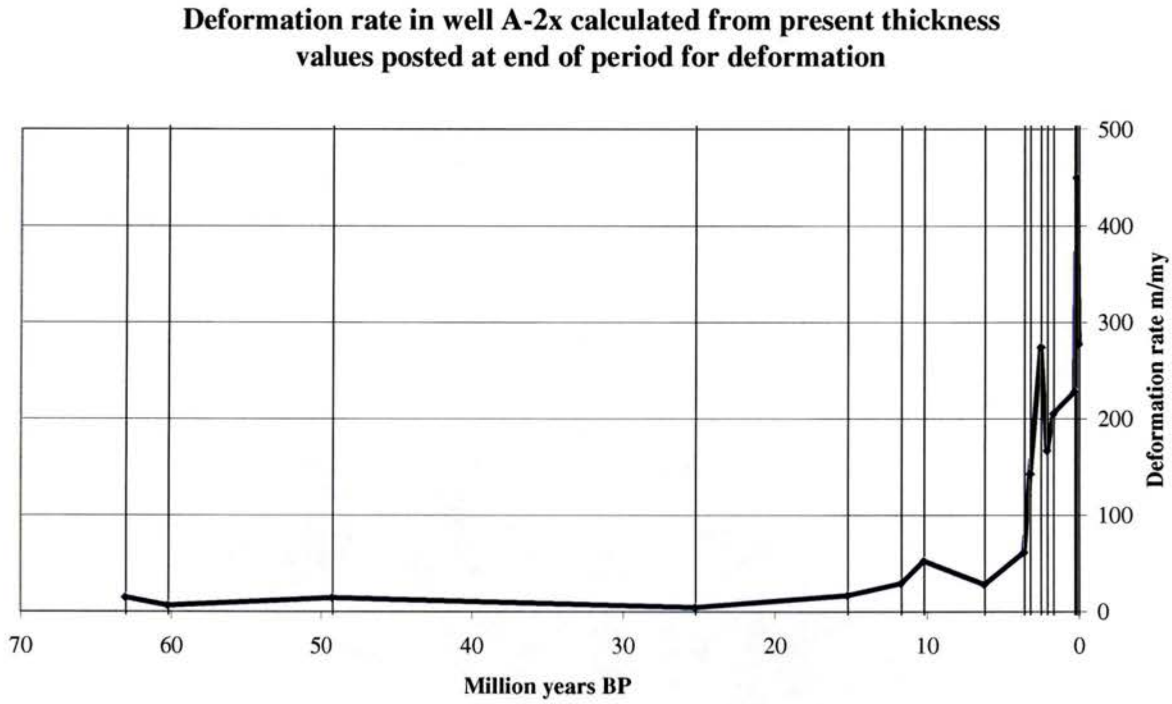

Fig. 12 – Development of the deformation rate as calculated from the present sediment thickness in well A-2x and the dating of the horizons. The high rates at the most recent burial is clearly seen although the exact values depend on the dating of horizons.

Conclusion

The major growth of the Kraka Structure terminated in the Lower Pliocene (before 3.6 MA BP). The deformation history from 3.6 MA BP to recent is dominated by regional subsidence (and/or tectonic tilting), occasionally with shorter intermittent intervals of structural growth of the Kraka and Dan domes. Moreover, the structural growth of the two salt structures are not simultaneously within the investigated time span.

A significant shift in the regional deformation trend is seen around 3.2 MA BP (early Upper Pliocene time). The orientation of the deformation field changes orientation from an easterly to a westerly subsidence. This shift in subsidence pattern could very well be caused by regional tectonic movements.

Implications for the fracture pattern

Assuming that "young" fractures have a better chance of avoiding cementation and thereby stay open in a reservoir, it is reasonable to assume that the latest deformation history is of most interest when dealing with open fractures in a reservoir. Based on this assumption, and the fact that major domal uplift in the Kraka area ceased around 3.6 MA BP, it is likely that the open fractures of the Kraka Field chalk reservoir originates from regional stress fields, rather than from local stress fields originating from domal uplifts. This would imply that local variations in the fracture orientation were insignificant (Salinas *et al.* 1994).

A prediction of fracture orientation based on the deformation fields, can only be estimated with considerable uncertainty. In the deformation fields described previously the overall strike of the deformation fields is NS. It is therefore to be expected that one of the major fracture/fault orientations to strike approx. NS.

Geodynamic reservoir modelling

The burial history of the Kraka area will be used to guide the development of reservoir parameters in the chalk section through time. Therefore some important decisions must be made even if only sparse data exists.

1. The porosity of the chalk will be modified according to the relation between effective stress and porosity as it has been developed from different types of data including deep sea drilling data (Lind 1993). This relation is monitored in time in combination with the effect from invasion of hydrocarbons that is assumed to halt the diagenetic reduction of the porosity.
2. The effective stress is modelled in time via the overpressure development following the sealing by the Mid-Miocene section. It should be noted that the estimations of overpressure can vary in the cited references for the same field depending on method for generation.
3. The permeability is modelled as a function of the porosity. The relation between porosity and permeability is well documented for a wide range of porosities (from more than 50%).
4. The capillary pressure function is modelled via its correlation with porosity (Engstrøm 1995).
5. Some basic principles for maturation and migration timing is obtained (Andersen *et al.* 1998).
6. The entry of hydrocarbons into the chalk section is modelled as an injection process, where the timing and rate is monitored.
7. The entry (injection) point for the hydrocarbons must be determined either as a low flank position, or combined with a lead point due to a fault or fracture zone that has acted as a corridor for migration.
8. The timing of the start of entry is depending on a) maturity timing of the source rock, b) travel distance and velocity from the source rock to the injection point in the reservoir model.
9. Fluid characteristics and the sequence of gas/oil phase entry.
10. In connection with the migration timing and the burial effect on the hydrocarbons, the temperature development in the chalk reservoir section over time must be modelled. This is to asses whether the temperature has any impact on the PVT behaviour of the reservoir fluids.
11. The influence from a possible regional hydrodynamic gradient. The gradient has been suggested to be in the order of 14 psi/km causing flow in the aquifer. The gradient is suggested to be caused by the maximum burial in the Ekofisk area, with the porewater being able to escape only through the regionally continous chalk aquifer, ultimately surfacing at the chalk outcrops in England, France and the subcrops in Holland, Germany and Denmark (Engstrøm in (Andersen 1997)).

Additional parameters and models for geodynamic flow modelling

The model for the depth-porosity is described as a simple monotonic model, with two type curves for normal and overpressured situations (Fig. 13). On the figure is shown data from chalk sediments from the ODP drillings.

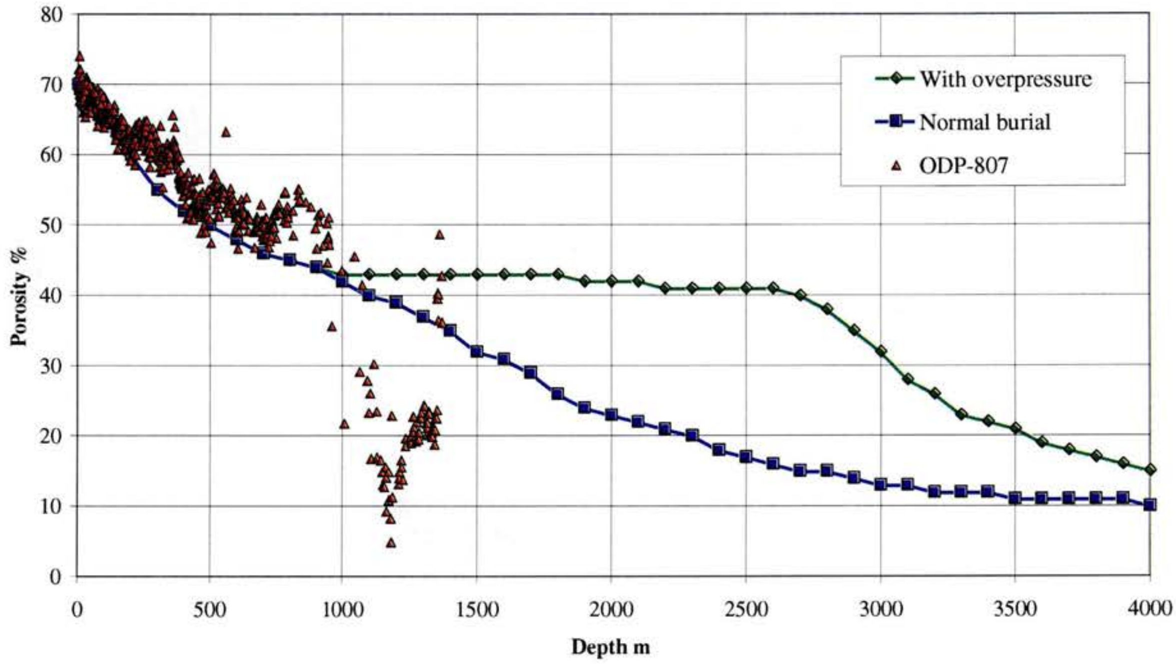

Fig. 13 – Depth-Porosity relation.

Transferred to the M8x situation, the time-porosity development is described (Fig. 14).

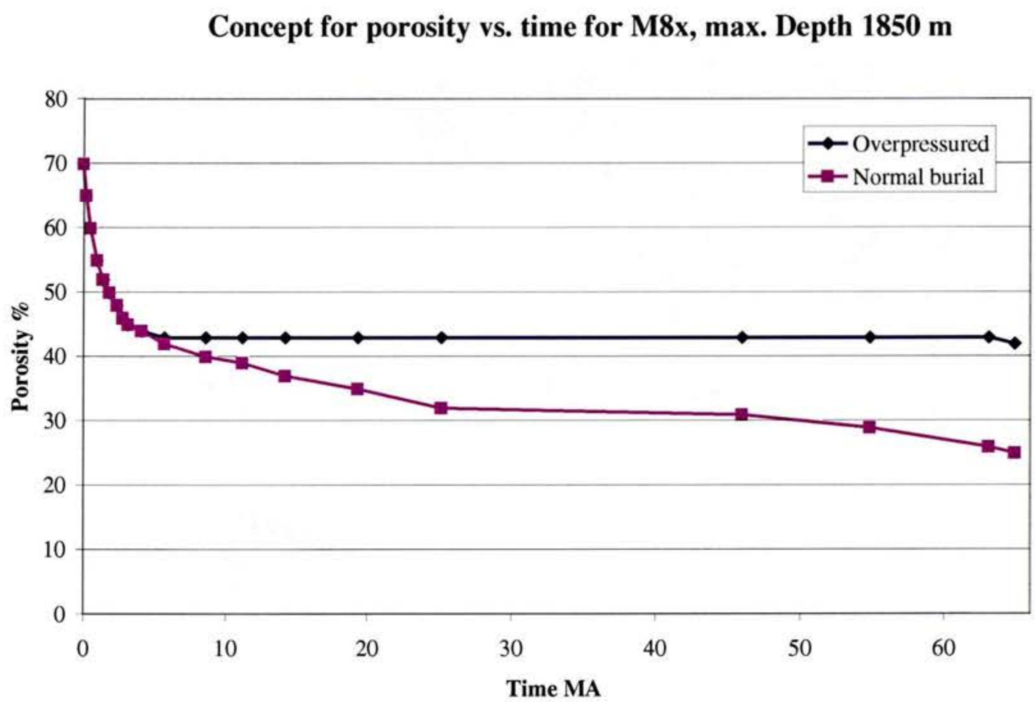

Fig. 14 – Time-porosity relation for well M8x

When this trend is converted to effective stress, a simpler solution is derived (Fig. 15).

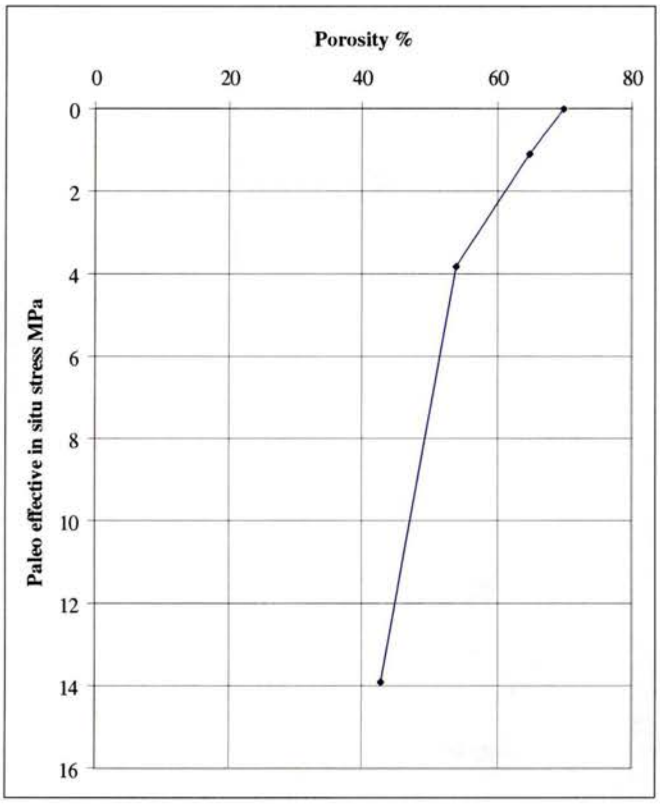

Fig. 15 – Porosity-effective stress (Gommesen & Fabricius 2001).

For the reservoir properties the porosity-permeability trend is obtained from the core data from the Dan Field, showing two distinct trends for the Maastrichtian and the Danian sections respectively (Fig. 16). This has to be further confirmed with data from the Kraka field itself.

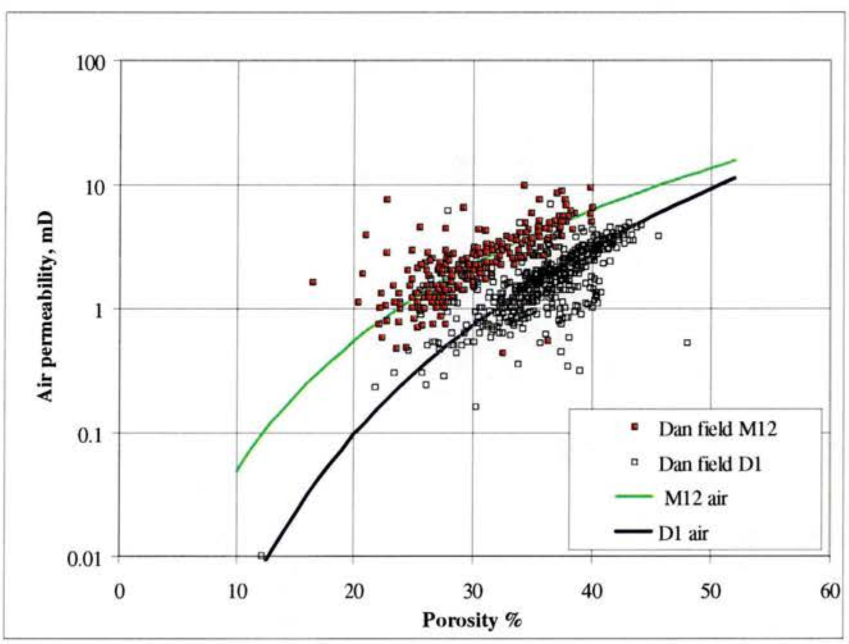

Fig. 16 – Porosity-permeability core data from wells in the Dan Field.

For the flow simulation is needed also the temperature development. This is assumed to be a simple linear relation with an end-point at the present day reservoir temperature in the A-2x well (Fig. 17).

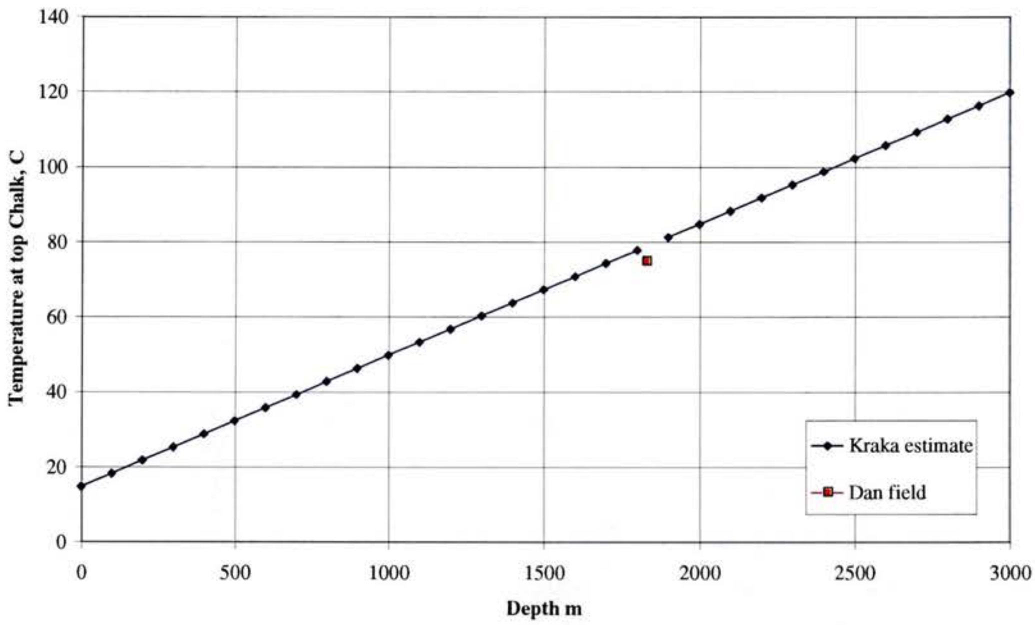

Fig. 17 – Depth/temperature function for the Kraka area.

Appendix

table 1

Well spud point UTM coordinates, spud date and well segment naming

630547.3	6141901.0	1966	27/08-1966	A-1X
630445.1	6142082.0	1967	30/07-1967	A-2X
631705.5	6141713.0	1989	02/05-1989	A-4
631705.5	6141713.0	1989	21/12-1989	A-4H
631705.3	6141714.0	1989	20/06-1989	A-5
631705.3	6141714.0	1989	23/07-1989	A-5H
631705.3	6141714.0	1994	13/08-1994	A-5HI
631704.6	6141712.0	1992	22/05-1992	A-6
631704.6	6141712.0	1992	16/06-1992	A-6A
631704.6	6141712.0	1992	28/06-1992	A-6I
631704.6	6141712.0	1992	12/07-1992	A-6II
631706.0	6141712.0	1993	11/03-1993	A-7
631706.0	6141712.0	1993	28/03-1993	A-7A
631706.0	6141712.0	1993	06/04-1993	A-7B
631706.0	6141712.0	1993	11/04-1993	A-7C
631706.0	6141713.0	1994	27/04-1994	A-8
631706.0	6141713.0	1994	02/06-1994	A-8I
631698.6	6141711.0	1994	22/06-1994	A-9
631726.8	6140735.0	1984	31/01-1984	ANNE-3
631726.8	6140735.0	1984	16/02-1984	ANNE-3A
631698.6	6141711.0	1997	16/03-1997	A-10P
631698.6	6141711.0	1997	12/04-1997	A-10
631698.6	6141711.0	1997	23/04-1997	A-10A
631698.6	6141711.0	1997	27/04-1997	A-10B
631698.6	6141711.0	1997	29/04-1997	A-10C

The A-10 well is released from confidentiality mid 2002.

For establishing a stratigraphy, seismic reflectors have been mapped, tied to the well data and dated. The post-chalk section has been divided into 14 layers. In Table 2 are listed the horizons, the layers and the dating of the horizons. The depths to the horizons in the A-2X well are listed also.

The last column indicates whether the horizons have been recognised and interpreted from the 3D seismic survey. The subdivisions are based on sonic logs and density logs. The further subdivision between the Top Overpressure and Tertiary D horizons was required in order to make it possible to simulate the varying sedimentation rates during that period (Olsen 1993). The listing of two top overpressure horizons in the table refer to the sonic log pick, and the seismically interpreted top overpressure location, respectively.

Table 2

Kraka-94 *data and maps*				**Well data A-2x**				Unikort	Zmap		
Horizon	**Layer**	**Dating** MA BP	**Time-interva** my	**Depth** ft TVD	**Interval thickness** ft	**Depth** m TVD	**Interval thickness** m	**Paleo topchalk-map**	**Data file with paleodepth**	**deformation-map**	
Seabed		0		145		44		tctday	fiftday.dat		
	Qua 3		0.17		155		47			def08	
Quarternary B		0.17		300		91		tcp08	fif08.dat		
	Qua 2		0.13		192		59			def07	
Quarternary A		0.3		492		150		tcp07	fif07.dat		
	Qua 1		1.4		1050		320			def06	
Top Tertiary		1.7		1542		470		tcp06	fif06.dat		
	Tert 5		0.4		270		82			def05	
Tertiary A		2.1		1812		552		tcp05	fif05.dat		
	Tert 4		0.4		220		67			def04	
Tertiary B		2.5		2032		619		tcp04	fif04.dat		
	Tert 3		0.7		630		192			def03	
Tertiary C		3.2		2662		811		tcp03	fif03.dat		
	Tert 2		0.4		188		57			def02	
Tertiary D		3.6		2850		869		tcp02	fif02.dat		
	Tert 1		2.6		529		161				
Top Lower CEN5		6.2		3379		1030					
	Lower cen5		4		378		115			def01	
Top Overpressure (log)		10.2		3757		1145					
	Upper Overp.		1.5		261		80				
Top Overpr. (seismic)		11.7		4018		1225		tcp01	fif01.dat		
	Upper Cen4		3.5		339		103			def10(iso)	
Top Lower CEN4		15.2		4357		1328		tcp10	fif10.dat		
	Lower Cen4		10		564		172			def11(iso)	
Top CEN3		25.2		4921		1500		tcp11	fif11.dat		def00
	Cen3		24		378		115				
Top CEN2		49.2		5299		1615				def12(iso)	
	Cen2		11		533		162				
Top Chalk		60.2		5832		1778					
	Danian 1		2.8		64		20				
Top Danian 2		63		5896		1797					
	Danian 2		2		101		31				
Top Maastrichtian		65		5997		1828					
	Maastr.+				1125		343				
Base Chalk				7122		2171					

Table 2 lists the horizons interpreted in the seismic mapping, dating, duration and thickness of the units, naming of data-files. The maps of top chalk and deformations listed do not necessarily match the thickness measures in the listed well, since the maps are made from decompacted data and some are partly created artificially. Table 2 is compiled from earlier work (Salinas *et al.* 1994), with addition of list of map names in this study.

Table 3 lists the average densities of the layers in 4 wells. The densities are measured from density logs where present, otherwise data from other Dan Field wells have been used (Olsen et. al, 1993).

Table 3

Layer	Density g/cm3				Interval velocity
	A-2X	Anne-3	A-5P	M-9X	Ft/sec
Qua 3	1.89	1.89	1.89	1.89	5498
Qua 2	1.94	1.94	1.94	1.90	5843
Qua 1	1.94	1.94	1.94	1.94	6313
Tert 5	2.00	2.00	2.00	2.00	6087
Tert 4	2.00	2.00	2.00	2.00	7241
Tert 3	2.00	2.00	2.00	2.00	6493
Tert 2	2.00	2.00	2.00	2.00	6387
Tert 1	2.18	2.18	2.18	2.18	7318
Lower Cen5	2.17	2.19	2.17	2.19	
Upper Overp.	2.06	1.98	2.06	2.00	
Upper Cen4	1.97	1.93	2.00	1.93	6983
Lower Cen4	2.01	1.97	2.05	1.97	6946
Cen3	2.06	2.03	2.10	2.04	
Cen2	2.07	2.05	2.06	2.10	
Danian 1	2.14	2.19	2.15	2.17	
Danian 2	2.27	2.25	2.25	2.31	
Maastr.+	2.37	2.37	2.37	2.37	

Table 4

Overburden and reservoir pressure gradients, pore pressure and depth information for the chalk reservoir interval. The hydrostatic pressure assumes a brine gradient of 10.5 kPa/m. Table supplemented but mostly reproduced from (Andersen 1995).

Field	Gradients KPa/m Over-burden	KPa/m Brine	KPa/m Normal effec-tive	KPa/m Reser-voir	Pore pres-sure MPa	At depth m	Ref.	Hydros tatic press. MPa	Over-pres-sure MPa
Dan/Kraka Dan	-	-	10.1	(6.6 ref A)	26.2 26.339 (initial press)	1890	B F	19.8	6.4
Eldfisk	20.6	10.5	10.1	15.6	47	2865	C	30.1	16.9
Ekofisk	-	-	10.1	15.5	48.5	3170	D	33.3	15.2
Valhall	20.1	-	9.6	6.3	44.5	2400	E	25.2	19.3
	-	-	-	-	46.4	2700	B	28.4	18.0

References: A.(Thomasen & Jacobsen 1994), B.(Childs & Reed 1975), C.(Michaud 1985), D.(Pekot & Gersib 1985), E.(Munns 1985), F.(Jørgensen 1993).

Table 5

Porosity and depth with calculated stresses, and "effective" depth. Overb. Is the overburden stress. Table reproduced from (Andersen 1995).

Field	Ref.	Depth m	Porosity %	Pressure	MPa	**Effective**	Effective
				Overb	Pore	**Overb**	Depth
Dan/Kraka	1	1814	40	37.3	25.7	**11.6**	1154
		1890	25	38.9	26.2	**12.7**	1260
Eldfisk	2	2820	43	58.1	46.3	**11.8**	1165
		2990	27	61.6	49.0	**12.6**	1249
		3040	24	62.6	49.7	**12.8**	1274
Ekofisk	3	3050	35.5	62.8	46.6	**16.1**	1601
		3260	18	67.1	49.9	**17.2**	1707
		3350	26.5	69.0	51.3	**17.7**	1752
		3400	21.5	70.0	52.1	**17.9**	1777
Valhall	4	2400	46	48.3	44.5	**3.8**	395
		2700	32	54.3	46.4	**7.9**	825

Table is reproduced from table 2.2 in (Andersen 1995)

References: 1.(Childs & Reed 1975), 2.(Maliva *et al.* 1991), 3.(Scholle 1977), 4.(Munns 1985).

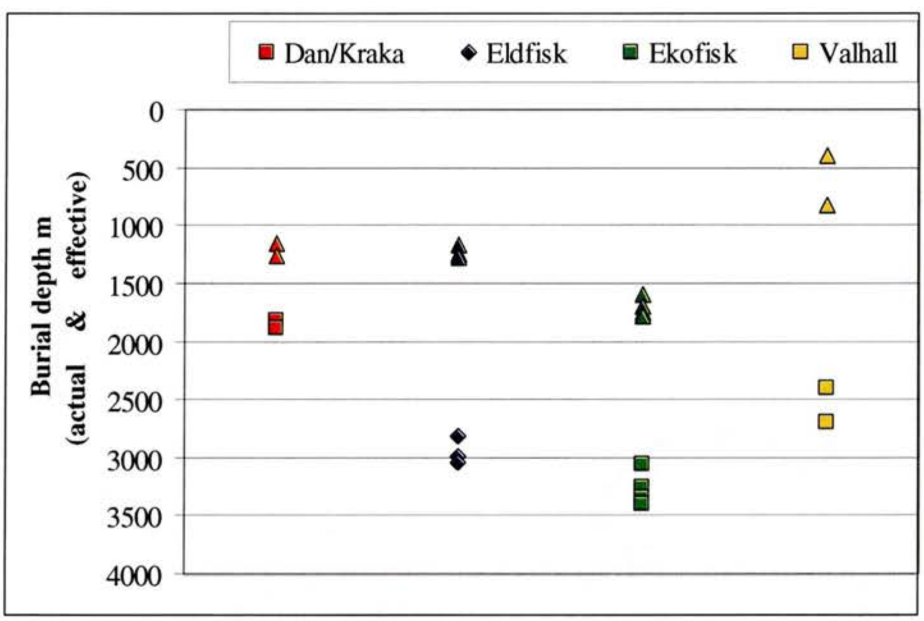

Figure A1: Illustration of the data in Table 5 of actual depth of reservoirs and the effective depth compensated for the overpressure.

Table 6
Mapped horizons and their corresponding TWT at the A-2X and M-9X well locations (Salinas *et al.* 1994).

Well	A-2X	M-9X
Horizon	TWT in msec	TWT in msec
1. Quaternary B	116	110
2. Quaternary A	182	174
3. Top Tertiary	508	500
4. Tertiary A	598	592
5. Tertiary B	664	650
6. Tertiary C	854	800
7. Tertiary D	906	862
8. Top Overpressure (seismic)	1222	1246
9. Top Lower Cen 4	1332	1366
10. Top Chalk	1758	1886
11. Top Maastrichtian	1784	1912
12. Base Chalk	1958	2138

References

Andersen, C., Bidstrup, T., Dahl, B., Ineson, J.R., Lomholt, S., Møller, J.J., Skaarup, N. & Thomsen, E. 1998: Secondary migration in the Central Trough. Danmarks og Grønlands Geologiske Undersøgelse Rapport 1998/51, 211 pp.

Andersen, M.A. 1995: Petroleum Research in North Sea Chalk, 179 pp. Stavanger, Norway: RF Rogaland Research and Joint Chalk Research Phase IV.

Andersen, P.M. 1997: Challenges of oil and gas production from low permeable Danish chalk reservoirs. 18th International Workshop and Symposium. International Energy Agency. Collaborative Project on Enhanced oil Recovery, Copenhagen, Denmark, August 31 - September 3, 1997, 21 pp.

Childs, F.B. & Reed, P.E.C. 1975: Geology of the Dan Field and the Danish North Sea Petroleum and the Continental Shelf of North-West Europe, 1, 429-438. New York: John Wiley & Sons, Inc.

Daniel, R.B. 2001: Pressure prediction for a Central Graben wildcat well, UK North Sea. Marine and Petroleum Geology 18(2), 235-250.

Danish Energy Agency 2001: Oil and gas production in Denmark. Annual Report 2000, 100 pp.

Engstrøm, F. 1995: A new method to normalize capillary pressure curves. 1995 International Symposium of the Society of Core Analysts, San Francisco, CA, USA, September 12-14, 1995, 12 pp.

Gommesen, L. & Fabricius, I.L. 2001: Dynamic and static elastic moduli of North Sea and deep sea chalk. Phys. Chem. Earth (A) 26(1-2), 63-68.

Jørgensen, L.N. 1993: Dan Field – Denmark. Central Graben, Danish North Sea. In: Beaumont, E.A. & Foster, N.H. (eds): Atlas of Oil and Gas Fields, 199-215. Tulsa: American Association of Petroleum Geologists

Jørgensen, L.N. & Andersen, P.M. 1991: Integrated Study of the Kraka Field SPE 23082. 1991 Offshore Europe Conference, Aberdeen, September 3-6, 9 pp.

Krogsbøll, A., Foged, N., Hansen, C.F., Zinck-Jørgensen, K., Christensen, H.F. & Jepsen, J. 1995: Modelling of stresses and fractures in a reservoir. 2 EFP-93 Final Report, 68, Copenhagen, Denmark.

Lind, I. 1993: Stylolites in chalk from Leg 130, Ontong Java Plateau. Proc. ODP Sci. Results 130, 445-451.

Maliva, R.G., Dickson, J.A.D. & Råheim, A. 1991: Modelling of chalk diagenesis (Eldfisk Field, Norwegian North Sea) using whole rock and laser ablation stable isotopic data. Geological Magazine 128, 43-49.

Megson, J.B. 1992: The North Sea Chalk Play: Examples From the Danish Central Graben. In: Hardman, R.F.P. (ed.): Exploration Britain: Geological Insights For the Next Decade 67., 247-282.: Geological Society Special Publication

Michaud, F. 1985: Eldfisk. In: Spencer, A.M. (ed.): Geology of the Norwegian Oil and Gas Fields, 89-105. Stavanger: Graham & Trotman

Munns, J.E. 1985: The Valhall Field: A Geological Overview. Marine and Petroleum Geology 2, 23-43.

Olsen, A. 1993: Further development of a mathematical model to simulate fracturing in chalk reservoirs. DGU Service Report 3 - 1993.

Pekot, L.J. & Gersib, G.A. 1985: Ekofisk. In: Spencer, A.M. (ed.): Geology of the Norwegian Oil and Gas Fields, 73-87. Stavanger: Graham & Trotman

Salinas, I., Madsen, L., Fabricius, H., Krogsbøll, A., Zinck-Jørgensen, K. & Abatzis, I. 1994: Evaluation of the Kraka Field. DGU Service Report 21 - 1994.

Scholle, P.A. 1977: Chalk diagenesis and its relation to petroleum exploration: Oil from chalks, a modern miracle. American Association of Petroleum Geologists Bulletin 61(7), 982-1009.

Thomasen, J.B. & Jacobsen, N.L. 1994: Dipping Fluid Contacts in the Kraka Field, Danish North Sea. 69th SPE Annual Technical Conference and Exhibition, New Orleans, LA, 25-28 September 1994, 763-772 (SPE 28435).

Thomasen, J.B. & Larsen, F.P. 1994: A multidisciplinary study for development optimization in a fractured chalk field. Proceedings of the 14th World Petroleum Congress, Stavanger, Norway, 297-304. John Wiley & Sons.